

1

ИНСТИТУТ ЯДЕРНОЙ ФИЗИКИ  
СО АН СССР

O.V.Zhirov

ON THE EXISTENCE  
OF THE LOCAL THERMAL EQUILIBRIUM  
IN HIGH ENERGY HADRONIC COLLISIONS

ПРЕПРИНТ ИЯФ 79-1

Новосибирск



ON THE EXISTENCE OF THE LOCAL THERMAL EQUILIBRIUM  
IN HIGH ENERGY HADRONIC COLLISIONS

O.V.Zhirov

Institute of Nuclear Physics,  
630090, Novosibirsk 90, USSR

A b s t r a c t

As a direct check of the local thermal equilibrium the new universality condition for spectra of secondaries (dileptons and hadrons) is proposed. Its comparison with data, as well as different estimates of the "effective temperature" of secondaries allow us to determine the applicability limits of the thermodynamical description.

Some estimates of the equation of state of hadronic matter are obtained.



## INTRODUCTION

As was proposed in Ref. [1], the process of hadron-hadron collision can be divided into two stages. At the first (parton) stage we have hard collisions of the constituents of initial hadrons. After the production of many new quarks and gluons, their "mixing" and reaching the local thermal equilibrium we have the second stage, the hydrodynamical expansion, up to break-up to free hadrons at final temperature  $T_f \sim m_\pi$ .

For description of the first stage there exists a very successful approach, the Feynman's parton model [2], which is now getting considerable and profound development on the basis of the modern theory of strong interactions - quantum chromodynamics (QCD) [3,4]. This approach gives us the understanding of hadron production at high  $p_\perp$  and in the fragmentation region, where hard collisions should dominate. The Drell-Yan model [5] based on the parton picture describes rather well dilepton production with a large invariant mass ( $M \geq 5$  GeV) [6,7].

As<sup>it</sup> was shown in [1], for smaller dilepton masses and transverse momenta of particles the main contribution is given by the thermodynamical mechanism at the second stage. This mechanism provides the uniform explanation of the yields of leptons, dileptons,  $\gamma$ -quanta, and hadrons, as well as their transverse momentum distributions. This fact can be treated as an additional argument in favor of the thermodynamical description of the final state interaction.

It should be stressed that leptons and photons flying out of the system right away without any secondary interaction are the most convenient objects to explore the space-time picture



of the hadron-hadron collisions, as it was firstly pointed out by E.L. Feinberg [8].

This work is a further extension of the ideas proposed in [1,8] and is devoted to a more detailed study of the quark-gluon system at different stages of hydrodynamical expansion.

In chapter 2 we formulate the direct consequence of the local thermal equilibrium, namely the universality of the spectra of secondaries (dileptons and hadrons) as a function of "transverse mass"  $m_{\perp} = \sqrt{p_{\perp}^2 + M^2}$  and rapidity  $y = \frac{1}{2} \ln \frac{E + P_{\parallel}}{E - P_{\parallel}}$ . The universal dependence on  $m_{\perp}$  follows from the common thermal mechanism of large mass and large  $p_{\perp}$  production. The universality in  $y$ -dependence reflect the fact that the particles with the same  $m_{\perp}$  are formed simultaneously, and hence, their spectra formed by the same collective motion distribution should coincide.

Our comparison of this universality with experimental data (chapter 2), and also different estimates of "effective temperature" ( $T_{\text{eff}}$ )<sup>of</sup> production of the particles with the definite  $m_{\perp}$  (chapter 3) make it possible to distinguish three regions in particle production spectra: 1) the hard collision region ( $m_{\perp} \geq 5$  GeV) treatable by the parton model; 2) the intermediate region of "incomplete mixing" ( $m_{\perp} \sim (3-4) \cdot 5$  GeV), where both the parton and thermodynamical descriptions fail (e.g., different ways to estimate  $T_{\text{eff}}$  give different values); 3) the region of the local thermal equilibrium ( $m_{\perp} \lesssim (3-4)$  GeV), where all of these estimates agrees with each other and the thermodynamical description is quite adequate.

In chapter 4 we obtain some estimates of hydrodynamical sound velocity being the main parameter of the equation of state of hadronic (quark-gluon) plasma.

$$c^2 = \frac{dP}{d\varepsilon}$$

where  $P, \varepsilon$  are the pressure and the energy density, respectively. In addition to the available experimental data we here use the assumption of the so-called "frame independence symmetry" of hydrodynamical expansion [9]. Our values of  $c^2$  are in reasonable agreement with those obtained in the papers [10-12].

## 2. The universality of spectra

The universality of the particle production spectra as a function of transverse mass has been discussed earlier for mediate  $p_{\perp}$  ( $\lesssim 2-3$  GeV) hadron production [13]. The origin of such a universality is very simple - it is due to the same thermodynamical mechanism both for the mass production and for the formation of the transverse momentum distribution. The major attention in our analysis is paid to the study of the spectra of particles (e.g., dileptons), comparatively weakly interacting with the system and therefore leaving it without any secondary interaction. We show that as a consequence of the local thermal equilibrium the spectra of such particles are expressed via the universal function of transverse mass  $m_{\perp}$  and rapidity  $y$  of the observed particle.

Let us consider the production of some system  $X$  consisting of  $N$  such particles (usually  $N = 1, 2$ ; e.g., a pair of leptons or/and production of "direct"  $\Upsilon$  + gluon and so on). The production rate of system  $X$  per unit volume of plasma of temperature  $T$  is



$$\dot{W} = \int \sum_A d\gamma_A \exp\left(-\frac{E_A}{T}\right) |\langle A | M | X \rangle|^2 d\gamma_X (2\pi)^4 \delta^{(4)}(P_A - P_X) \quad (1)$$

where  $d\gamma_A$  is the element of the phase space volume of subsystem  $A$ , which is in the thermal equilibrium with the whole system (quark-gluon plasma) but  $A$  is supposed to turn into  $X$  entirely;  $\int d\gamma_A \exp\left(-\frac{E_A}{T}\right)$  is its Gibbs thermodynamical probability and  $\langle A | M | X \rangle$  is the amplitude of transition of  $A$  to  $X$ ,  $d\gamma_X = \prod_i \frac{g_i d^3 p_i}{2E_i (2\pi)^3}$  is the element of phase-space volume of  $X$ ,  $g_i$  is the statistical weight of its  $i$ -th constituent. Since  $E_A = E_X = E$ , from (1) we have

$$\frac{d\dot{W}}{d\gamma_X} = \exp\left(-\frac{E}{T}\right) \int \sum_A d\gamma_A |\langle A | M | X \rangle|^2 (2\pi)^4 \delta^{(4)}(P_A - P_X) \quad (2)$$

It is very convenient to connect eq.(2) with the rate of the inverse process, namely the decay of  $X$  into the system  $A$ . In the most interesting cases, the invariant mass  $M_X = \sqrt{(p_1 + \dots + p_n)^2} \gg T$ , the process occurs at small distances and the influence of plasma on the inverse process rate can be neglected. This allows us to replace this rate by the common decay rate of  $X$  into usual hadrons. If  $X$  is a single particle (say,  $\psi$ ), from eq.(2) one has

$$E \frac{d\dot{W}}{d^3 p} = \exp\left(-\frac{E}{T}\right) \cdot \frac{g_X M_X \Gamma(X \rightarrow \text{hadrons})}{(2\pi)^3} \quad (3)$$

where  $g_X = (2S_X + 1)$  and  $\Gamma$  are the statistical weight and the hadronic width of  $X$ . If  $X$  is the pair of light particles  $a, b$  ( $m_{a,b} \ll M$ ), instead of eq.(3) one gets

$$\begin{aligned} E_a E_b \frac{d\dot{W}}{d^3 p_a d^3 p_b} &= \exp\left(-\frac{E_a + E_b}{T}\right) \cdot \frac{2g_a g_b E_a E_b}{(2\pi)^6} \sigma(a b \rightarrow \text{hadrons}) = \\ &= \exp\left(-\frac{E}{T}\right) \frac{g_a g_b M_X^2 \sigma(a b \rightarrow \text{hadrons})}{2 (2\pi)^6} \end{aligned} \quad (4)$$

Let us consider now the case when  $X$  is a pair of leptons (dilepton).

1. Dileptons. From eq.(4) it is easy to obtain that

$$E \frac{d\dot{W}}{dM^2 d^3 p} = \exp\left(-\frac{E}{T}\right) \frac{\mathcal{L}^2}{24\pi^4} R(M^2) \quad (5)$$

where  $R(M^2) = \frac{\sigma(e^+e^- \rightarrow \text{hadrons})}{\sigma(e^+e^- \rightarrow \mu^+\mu^-)}$

Very convenient variables are the dilepton "transverse mass"  $m_\perp = \sqrt{M^2 + p_\perp^2}$  and its rapidity  $y = \frac{1}{2} \ln \frac{E + p_\parallel}{E - p_\parallel}$ . Integrating eq.(5) over time and space along the (hydrodynamical) system and neglecting the transverse collective motion, we obtain

$$E \frac{d\dot{W}}{dM^2 d^3 p} = \frac{\mathcal{L}^2}{24\pi^4} R(M^2) \sigma_{in} \int dt d^3 x \exp\left(-\frac{m_\perp \text{ch}(y - \hat{y}(x,t))}{\hat{T}(x,t)}\right) \quad (6)$$

Here  $\hat{T}(x,t)$  and  $\hat{y}(x,t)$  are the local temperature and rapidity of the collective motion,  $\sigma_{in}$  is the inelastic cross-section of initial hadrons. The expression (6) can also be presented in the more transparent form:

$$E \frac{d\dot{W}}{dM^2 d^3 p} = F(M^2) \cdot f(m_\perp, y) \quad (7)$$

which emphasizes a factorization of the specific dynamics of dilepton production process expressed by  $F(M^2) = \frac{\mathcal{L}^2}{24\pi^4} R(M^2)$  from the universal function

$$f(m_\perp, y) = \sigma_{in} \int dt d^3 x \exp\left(-\frac{m_\perp \text{ch}(y - \hat{y}(x,t))}{\hat{T}(x,t)}\right) \quad (8)$$

This function is a general characteristic of the hydrodynamical expansion independent of the invariant dilepton mass  $M$ . So, we find that the spectra of any thermodynamically produced par-



ticle is connected with the same universal function  $f(m_{\perp}, y)$  depending only on energy and, generally speaking, on the initial hadrons. It is worthy to stress that factorization (7) is a direct consequence of the microcanonical distribution in the phase space, which is assumed in eq.(1).

Factorization (7) is confirmed rather well by the recently measured dilepton spectra at  $\sqrt{s} = 21 \text{ GeV}$  [14]. In Fig.1  $\frac{1}{\sqrt{s}} \frac{d\sigma}{dm^2 dm_{\perp}^2 dy}$  is plotted as a function of the dilepton mass for different values of  $m_{\perp}$ <sup>1)</sup>. The data are in a reasonable agreement with the approximate constancy of  $R(M^2)$  in the nonresonance region  $M = 1.2 - 2.7 \text{ GeV}$ , while within the same interval of the normalization of data changes by several orders of magnitude<sup>2)</sup>.

Since in the nonresonance region  $F(M^2) \approx \text{const}$ , the inclusive dilepton cross section as a function of transverse mass  $m_{\perp}$  and rapidity  $y$  should be independent of  $M$  and be proportional to the same universal function  $f(m_{\perp}, y)$  (see eqs.(7),(8)).

1) The dilepton points (Fig.1) and the curves (Figs.2,3) are recalculated from the data parametrization [14]

$$\int_{M_1}^{M_2} dM E \frac{d\sigma}{dM d^3p} = A e^{-B p_{\perp}} \left(1 - \frac{2 p_{\perp}}{\sqrt{s}}\right)^C$$

in 7 intervals of dilepton mass,  $M = 0.65 - 3.5 \text{ GeV}$ .

2) It should be however noticed that at the same time the experimentally observed dilepton production in  $J/\psi$  region appears to be  $\sim 25$  times larger than it could be expected from the extrapolation of "nonresonance" data by eq.(6) (dotted line). Taking into account the recently measured large charm yields  $15 (G_{pp \rightarrow D+X} \sim 30-70 \mu\text{b})$ , this question deserves an additional study.

Shaded bands in Fig.2 show the scattering of curves corresponding to different values of  $M$  at fixed  $m_{\perp}$ . Note, that dileptons with larger values of  $m_{\perp}$  are distributed in narrower intervals of rapidity. As we shall see in chapter 3, with an increase of  $m_{\perp}$  the effective temperature of particle production is growing too. Hence, the dileptons with greater  $m_{\perp}$  are radiated at earlier stages of the hydrodynamical expansion. So, the  $M$ -independence of  $f(m_{\perp}, y)$  at different  $m_{\perp}$  is an evidence of the local thermal equilibrium at different stages of the expansion.

Fig.3 shows that such a  $M$ -independence (universality) of  $f(m_{\perp}, y)$  is valid at  $m_{\perp} \lesssim 3-4 \text{ GeV}$  and is strongly violated at  $m_{\perp} \geq 5 \text{ GeV}$ . Let us mention that in this region the main contribution is given by the hard collisions of the initial hadron constituents and the dilepton production is well described by the Drell-Yan model. On the other hand, Fig.4 shows that the scaling expected in the Drell-Yan model

$$M^3 \frac{d\sigma}{dM dy} \Big|_{y=0} = f(\tau), \quad \tau = \frac{M^2}{s}$$

is really valid only for heavy dileptons  $M \geq 3.9 \text{ GeV}$  (open points) and is strongly violated for light lepton pairs  $M \leq 2.7 \text{ GeV}$  (black points).

2. Hadrons with  $p_{\perp} = 1-4 \text{ GeV}$ . According to [1], their production is not the volume effect but the surface one. The particle flux through the side surface is

$$E \frac{dJ}{d^3p} = \frac{g_a p_{\perp}}{(2\pi)^3} \exp\left(-\frac{m_{\perp} c h y}{T}\right) \quad (9)$$

where  $g_a$  is the statistical weight of the particle. Neglecting the transverse collective motion and taking the system to be



a cylinder of radius  $r_0$  ( $\sim 1/m_\pi$ ) [1], we get:

$$E \frac{dG}{d^3p} = \frac{g_a P_\perp}{(2\pi)^3} \epsilon_{in} \int \exp\left(-\frac{m_\perp ch(y-\hat{y}(x,t))}{T(x,t)}\right) dS_\perp dt \approx$$

$$\approx \frac{g_a P_\perp}{(2\pi)^3} \epsilon_{in} \int \exp\left(-\frac{m_\perp ch(y-\hat{y}(x,t))}{T(x,t)}\right) \frac{dV}{2r_0} dt = \frac{g_a P_\perp}{2r_0 (2\pi)^3} f(m_\perp, y) \quad (10)$$

This estimate is good only for hadrons produced in the central region  $y \approx 0$ . [1]. Outside the central region, especially for hadrons with higher  $p_\perp$  corresponding to the early stage of the hydrodynamical expansion, the contribution of the front (back) surface of the system which has a thin disc shape at the beginning of expansion may be significant. In view of this, eq.(10) should be underestimated. Experimentally this should be observed as a noticeable increase of the dilepton-hadron ratio outside the central region at  $m_\perp \sim 2-3$  GeV.

The ratio of pions to dileptons in the central region, which is expected from eqs. (7) and (10), is plotted in Fig.5. Curves

$g_a = 1, 0.2$  correspond to the "leakage" of hadrons and quarks respectively [1]. The experimental data at  $\sqrt{s} = 21, 23$  GeV [14,16,17] show that for the hadrons with  $m_\perp = 1-2$  GeV it is possible to ascribe them to the "leakage" of hadrons but for higher  $m_\perp$  a more probable mechanism seems to be the "leakage" of quarks. Although this conclusion is not final (remind that both the pion and dilepton yields vary by several orders of magnitude and estimate (10) is rather crude), the relatively weak dependence of this ratio on  $m_\perp$  permits us to hope for their common (thermodynamical?) production mechanism.

### 3. The effective temperature

Let us now consider a few estimates of the effective production temperature of the particles with the definite transverse mass. These estimates can be made by expressing  $T_{eff}$  via the average energy and transverse momenta of quarks and gluons in various ways. In the case of the perfect thermal equilibrium all of them, of course, should coincide.

We confine ourselves to the effective temperature only for the particles produced in the central region ( $y = 0$ ) where the contributions of nonthermodynamical mechanisms are less important. As we have shown above, in this region the hadron (10) and dilepton (7) spectra can be expressed through the same function  $f(m_\perp, y)$  which characterizes the space-time picture of expansion.

Our first estimate of  $T_{eff}$  is obtained from the inclusive spectra of dileptons and hadrons. For  $m_\perp \gg T$  from eq.(8) we have the expression

$$\left. \frac{1}{T_{eff}} \right|_{y=0} = \epsilon_{in} \int d^4x \frac{1}{T(x,t)} \exp\left(-\frac{m_\perp ch(y-\hat{y}(x,t))}{T(x,t)}\right) \approx$$

$$\approx -\frac{2}{\partial m_\perp} \ln f(m_\perp, 0) - \frac{1}{2m_\perp} \quad (11)$$

A study of the dependence of  $T_{eff}$  on the dilepton invariant mass

$M$  at fixed  $m_\perp$  allows us to check the thermal equilibrium between longitudinal and transverse degrees of freedom. Indeed, for light dilepton ( $M \ll m_\perp$ ) as the final leptons, as the initial quarks fly almost in the same transverse direction and estimate (11) characterizes some "transverse temperature". In contrast, in heavy dilepton production ( $M \approx m_\perp$ ) the initial quarks



can fly in any direction and there are contributions of the "transverse" and "longitudinal" temperatures.

Another estimate of  $T_{\text{eff}}$  can be obtained from the dilepton data for  $\left. \frac{dG}{dM dy} \right|_{y=0}$  for dilepton "continuum". Integrating (7) over  $m_{\perp}$ , we get:

$$\left. \frac{dG}{dM dy} \right|_{y=0} = 2\pi M F(M^2) \int d^4x \exp\left(-\frac{Mch\hat{y}}{\hat{T}}\right) \cdot \left(\frac{\hat{T}}{ch\hat{y}} + \frac{\hat{T}^2}{Mch^2\hat{y}}\right)$$

for  $M \gg T$  one has

$$\frac{\partial}{\partial M} \left( \frac{1}{2\pi M F(M^2)} \left. \frac{dG}{dM dy} \right|_{y=0} \right) \approx f(m_{\perp}, 0) \quad (12)$$

and together with (11) we have independent estimate of  $T_{\text{eff}}$ .

Finally,  $T_{\text{eff}}$  can be estimated from the  $p_{\perp}$  distribution momenta:

$$T_{\text{eff}} = \frac{a_K C_K^2}{M [1 + b_K \left(\frac{C_K}{M}\right)^2]} \quad (13)$$

$$C_K \equiv \frac{\langle p_{\perp}^K \rangle}{\langle p_{\perp}^{K-1} \rangle}$$

The parameters  $a_K, b_K$  ( $K = 1+3$ ) are given in Table 1. Note that  $C_2, C_3$  are more convenient than  $C_1$  ( $\equiv \langle p_{\perp} \rangle$ ), because they are less sensitive to experimental uncertainties at small  $p_{\perp}$ .

The results obtained by eq.(11) from dilepton [14] and hadron [16] data at energies  $\sqrt{s} = 21, 23$  GeV are plotted in Fig.6. These estimates are in a sufficiently good agreement at  $m_{\perp} = 1+2$  GeV and slightly disagree at  $m_{\perp} \sim 3$  GeV. The estimate based on (13) and the  $\langle p_{\perp} \rangle$  of dileptons [14] at  $m_{\perp} \lesssim 2$  GeV agrees with (11) but at  $m_{\perp} > 2$  GeV it gives too low values of  $T_{\text{eff}}$  decreasing with an increase of  $m_{\perp}$ . Estimates based on (13) for  $K = 2, 3$  lead to higher  $T_{\text{eff}}$  and are in a rea-

sonable agreement with (11).<sup>3)</sup> Note that, according to the data [7],  $\langle p_{\perp}(M) \rangle \approx \text{const}$  for  $M \geq 5$  GeV in the hard collision region and  $T_{\text{eff}}$  (13) decreases with  $M$ . There remains unknown whether the abovementioned disagreement is a consequence of the experimental uncertainties for small  $p_{\perp}$  or it is connected with a lack of the local thermal equilibrium.

For higher energies  $\sqrt{s} = 53-63$  GeV,  $T_{\text{eff}}$  given by (11) for hadrons [16] and by (12) for dileptons [18] are also in reasonable agreement. At  $m_{\perp} \geq 5$  GeV the  $T_{\text{eff}}$  begins to grow very fastly with  $m_{\perp}$  being the evidence for the large contribution of hard collisions.

#### 4. Sound velocity

The essential parameter of the equation of state of quark-gluon plasma is the sound velocity:

$$c^2 = \frac{dP}{d\varepsilon} = \frac{S}{T} \frac{dT}{dS} \quad (14)$$

where  $S$  is the entropy density. A simple estimate for  $c^2$  can be obtained directly from the universal function  $f(m_{\perp}, y)$  characterizing a space-time picture of the expansion. For  $m_{\perp} \gg T$  from (8) one has

$$f(m_{\perp}, y=0) = \int dt d^2x_{\perp} dx_{\parallel} \exp\left(-\frac{m_{\perp} ch\hat{y}(x, t)}{\hat{T}(x, t)}\right) \approx$$

$$\approx \int dt d^2x_{\perp} \left(\frac{dx_{\parallel}}{d\hat{y}}\right)_{\hat{y}=0} \exp\left(-\frac{m_{\perp}}{\hat{T}}\right) \cdot \frac{\sqrt{2\pi\hat{T}}}{m_{\perp}}$$

3) The moments  $C_2, C_3$  are estimated from the experimental data parametrization obtained in [14].



Introducing [1]

$$\Phi(\tau) = \int dt d^2x_{\perp} \left( \frac{dx_{\perp}}{d\hat{q}} \right)_{\hat{q}=0} \delta(\tau - \hat{T}(x, t))$$

we obtain

$$f(m_{\perp}, 0) = \sqrt{\frac{2\pi}{m_{\perp}}} \int_{T_f}^{T_i} dT \Phi(\tau) T^{1/2} \exp\left(-\frac{m_{\perp}}{T}\right) \quad (15)$$

Under assumption that the hydrodynamical expansion in the central region is isoentropical and has the so-called "frame independence symmetry" [9], we get (see Appendix):

$$\Phi(\tau) = \text{const} \cdot T^{-(1 + \frac{2}{c^2})} \quad (16)$$

Substituting (16) in (15), one has

$$f(m_{\perp}, 0) = \text{const} \cdot \int_{T_f/m_{\perp}}^{T_i/m_{\perp}} dx \cdot x^{-(1 + \frac{2}{c^2})} \exp\left(-\frac{1}{x}\right) \quad (17)$$

The main contribution to this integral is given by the region  $(T^* - \delta T, T^* + \delta T)$ , where

$$T^* = \frac{2m_{\perp}c^2}{4 + c^2}; \quad \frac{\delta T}{T^*} = \sqrt{\frac{2c^2}{4 + c^2}} \quad (18)$$

The most useful case is that wherein the contributions of the limits themselves  $T \sim T_i, T \sim T_f$  are negligible. The reason is that near the upper limit ( $T \sim T_i$ ) the estimate (16) fails because of viscosity, and near the lower limit ( $T \sim T_f$ ) there is no simple connection between  $f(m_{\perp}, y)$  and the inclusive spectra of dileptons and hadrons. In this case, from (17) we have

$$f(m_{\perp}, 0) \sim m_{\perp}^{-\frac{2}{c^2}}$$

Whence,

$$c^2 = - \frac{2}{m_{\perp} \frac{2}{m_{\perp}} \ln f(m_{\perp}, 0)} \quad (19)$$

The criterion of applying this estimate is the independence  $T^*$  (almost the same as  $T_{\text{eff}}$  (11)) on the energy of initial hadrons. This independence is a direct consequence of the abovementioned "frame independence symmetry". Fig.6 shows that such an approximate independence takes place for  $m_{\perp} \sim 1-2$  GeV at  $\sqrt{s} = 23-63$  GeV. One can use the dilepton and hadron data at  $m_{\perp} \sim 2$  GeV to obtain  $c^2 = 0.22-0.24$  for  $T^* \sim 0.21-0.23$  GeV. This is somewhat higher than the value  $c^2 = 0.2$  obtained in [10] for imperfect hadron gas and is lower than  $c^2 = 1/3$  calculated in [11] for quark-gluon plasma within the high temperature limit. The close values  $c^2 \approx 0.2-0.25$  were obtained in the independent analysis of low  $p_{\perp} (\leq 1 \text{ GeV})$  spectra of secondaries [12].

Fig.7 shows the dependence of  $c^2$  on  $T$  and also on the energy of initial hadrons  $\sqrt{s}$ , which has been calculated from the data in [16] ( $\sqrt{s} = 23-63$  GeV). Although the applicability of (19) in the whole region is very questionable one can hope that in the "plato" region these estimates are reasonable. The fast increase at  $T \sim m_{\perp}$  should be apparently connected with the large contribution of the lower limit  $T \sim T_f$  to (17) and means that the estimate (19) here fails.

## 5. Conclusion

The analysis of experimental data allows us to divide the spectra of the produced particles into three regions:

- 1) The region of hard collisions ( $m_{\perp} \geq 5$  GeV) where distributions



of partons are determined by the structure functions of the initial hadrons.

2) The region of "incomplete mixing" ( $m_{\perp} \sim (3-4)+5$  GeV).

In this region the scaling expected in the parton model is strongly violated because of repeated interactions of newly produced quarks and gluons. The local thermal equilibrium is also absent, so that different estimates of  $T_{\text{eff}}$  give different values.

3) The region of the local thermal equilibrium (3-4) GeV.

All of the  $T_{\text{eff}}$  estimates are the same, the spectra of particles in the central region are connected with the same function  $f(m_{\perp}, y)$ .

The more precise limits of the thermodynamical description may be determined in further studies of the universality of spectra. The most convenient way is the detailed check of the factorization (7) of the dynamical factor  $F(M^2)$  from the universal function  $f(m_{\perp}, y)$ .

Another possibility is to study different estimates of  $T_{\text{eff}}$  for various  $m_{\perp}$ . Most promising is the comparison of estimates (11), (12) obtained from inclusive spectra of dileptons and hadrons with estimates (13) obtained from the  $p_{\perp}$  distribution of dileptons. Very interesting information could be obtained here from more accurate experimental data for  $\langle p_{\perp} \rangle$ ,  $\langle p_{\perp}^2 \rangle$  and higher moments of  $p_{\perp}$  distribution of dileptons with  $M = 2+5$  GeV.

The author is much indebted to E.V. Shuryak for numerous and valuable discussions.

## Appendix

Let us consider the isoentropic one-dimensional hydrodynamical expansion with the "frame independence symmetry". The entropy density  $S$  should depend only on the proper time  $\tau$  of a given part of the hydrodynamical system [9]:

$$S = \frac{\text{const}}{\tau}$$

One may use  $S = T^{1/c^2}$  to have

$$T \propto \tau^{-c^2}$$

Since  $(\frac{dX_{II}}{dy}) \propto \tau$ , we obtain

$$\Phi(\tau) = \int d\tau' (\frac{dX_{II}}{dy}) \delta(\tau - \tilde{\tau}(\tau')) \propto \tau^{-(\frac{2}{c^2} + 1)}$$



References

1. E.V.Shuryak. Yadernaya Fizika, 28, 796, 1978; Phys.Lett., 78B, 150, 1978.
2. R.P.Feynman. Photon-hadron interactions. Benjamin inc.,1972;  
R.P.Feynman, R.D.Field, G.C.Fox. Nucl.Phys., B128, 1, 1977;  
R.D.Field, R.P.Feynman, Phys.Rev. D15, 2590, 1977.
3. B.L.Combridge, J.Kripfganz, J.Ranft. Phys.Lett., 70B, 234,  
1977; R.Gutler, D.Sivers. Preprint ANL-HEP-PR-77-40.
4. Yu.L.Dokshitzer, D.I.D'yakonov, C.I.Troyan. Lectures of 13  
LIYaF Winter School, High Energy Physics, p.3, 1978; Phys.  
Lett. 78B, 290, 1978.
5. S.D.Drell, T.M.Yan. Phys.Lett., 24, 181, 1970.
6. D.C.Hom et al. Phys.Rev.Lett., 37, 1374, 1976.
7. D.M.Kaplan et al. Phys.Rev.Lett., 40, 435, 1978.
8. E.L.Feinberg. Izvestiya Akad. Nauk SSSR, ser.fiz., 26, 622,  
1962; Nuovo Cimento, 34A, 391, 1976.
9. C.B.Chiu, E.C.G.Sudarshan, Kuo-hsiang Wang. Phys.Rev. D12,  
902, 1975.
10. O.V.Zhirov, E.V.Shuryak. Yadernaya Fizika, 21, 861, 1975.
11. E.V.Shuryak, ZhETF, 74, 408, 1978.
12. B.Anderson, G.Jarlskog, G.Damgaard. Nucl.Phys., B112, 413,  
1976.
13. E.V.Shuryak. Yadernaya Fizika, 20, 549, 1974.
14. J.G.Branson et al. Phys.Rev.Lett., 38, 1331, 1977, *ibid.*1334.
15. A.G.Clark et al. Phys.Lett., 77B, 339, 1978.
16. K.Eggert et al., Nucl.Phys., B98, 93, 1975.
17. B.Alper et al. Nucl.Phys., B100, 237, 1975.
18. A.G.Clark et al. Nucl.Phys., B142, 29, 1978.

Table 1

$K$	1	2	3
$a_K$	0.62	0.38	0.27
$b_K$	0.45	0.32	0.31



FIGURE CAPTIONS

Fig.1 The factorization (7) of dependences on transverse  $m_{\perp}$  and invariant  $M$  dilepton masses. The points correspond to the values of  $m_{\perp} = 1.4, 1.8, 2.25, 2.7, 3.3$  GeV. The data demonstrate  $F(M^2) \approx \text{const}$  for  $M = 1.1-2.7$  GeV. In the  $J/\psi$  region the experimental yield of dileptons is approximately 25 times larger than that expected from (6) (dotted line).

Fig.2 The universality of "kinematical" function  $f(m_{\perp}, y)$ . The different curves correspond to  $M = 1.23, 1.65, 2.1, 2.5$  GeV. For comparison, there is plotted a dashed curve, which corresponds to inclusive spectra of dilepton production in  $J/\psi$  region ( $M = 3.1$  GeV) multiplied by the factor  $3 \cdot 10^{-2}$ .

Fig.3 Inclusive dilepton spectra as a function of  $m_{\perp}$ . Data are taken from [14] ( $\sqrt{s} = 21$  GeV) and [7] ( $\sqrt{s} = 28$  GeV).

Fig.4  $M^3 \frac{dG}{dM dy}$  for dileptons as a function of scaling variable  $\tau = \frac{M^2}{s}$ . The data are taken from [14] ( $\sqrt{s} = 21$  GeV) [7] ( $\sqrt{s} = 28$  GeV) and [18] ( $\sqrt{s} = 53, 63$  GeV). The solid curve shows a Drell-Yan model fit [7]. The dashed curves are drawn guide the eye and illustrate the scaling violation in the low-mass region.

Fig.5 The ratio of  $\bullet - \pi^-$  and  $\circ - \pi^0$  to dileptons.  $\beta_a = 1, 0.2$  correspond to the "leakage" of hadrons and quarks, respectively. The dilepton cross sections  $\frac{dG}{\pi dM^2 dm_{\perp}^2 dy}$  are calculated from the obtained in [14] parametrization of experimental data.

Fig.6 The effective temperature of particle production as a function of  $m_{\perp}$ . The solid curves correspond to hadron data [16], the dashed curve corresponds to dilepton data at  $\sqrt{s} = 21$  GeV [14] (eq.(11)), the dotted one to dilepton data at  $\sqrt{s} = 53-63$  GeV [18] (eq.(12)). The points are calculated from  $c_k = \langle P_{\perp}^k \rangle / \langle P_{\perp}^{k-1} \rangle$  (eq.(13)):  $\bullet - k=1, \circ - k=2, * - k=3$ .

Fig.7 The  $C^2$  dependence on  $T^*$ . Different solid lines correspond to different values of  $\sqrt{s}$ . The dashed lines are isolines  $m_{\perp} = \text{const}$ .



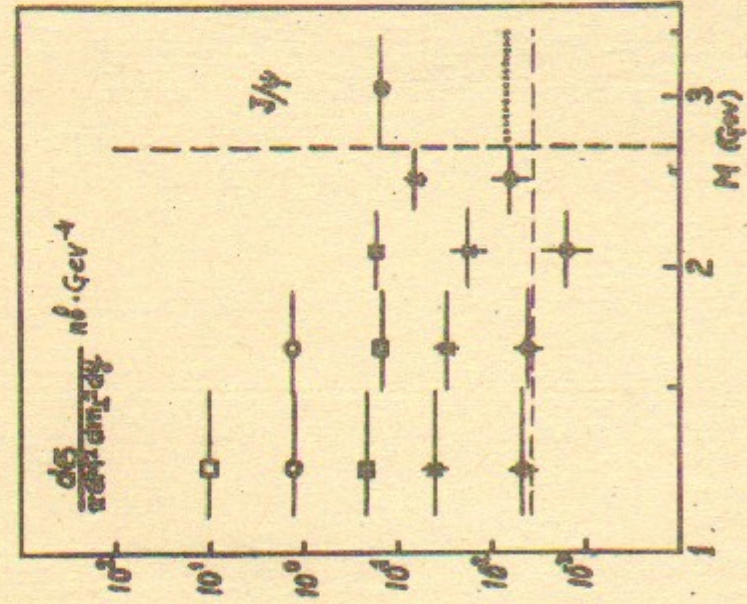


Fig. 1

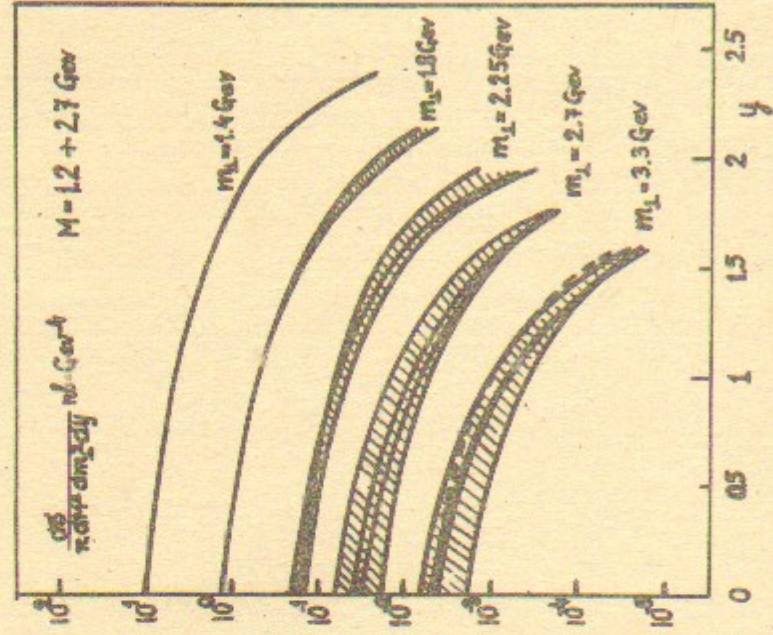


Fig. 2

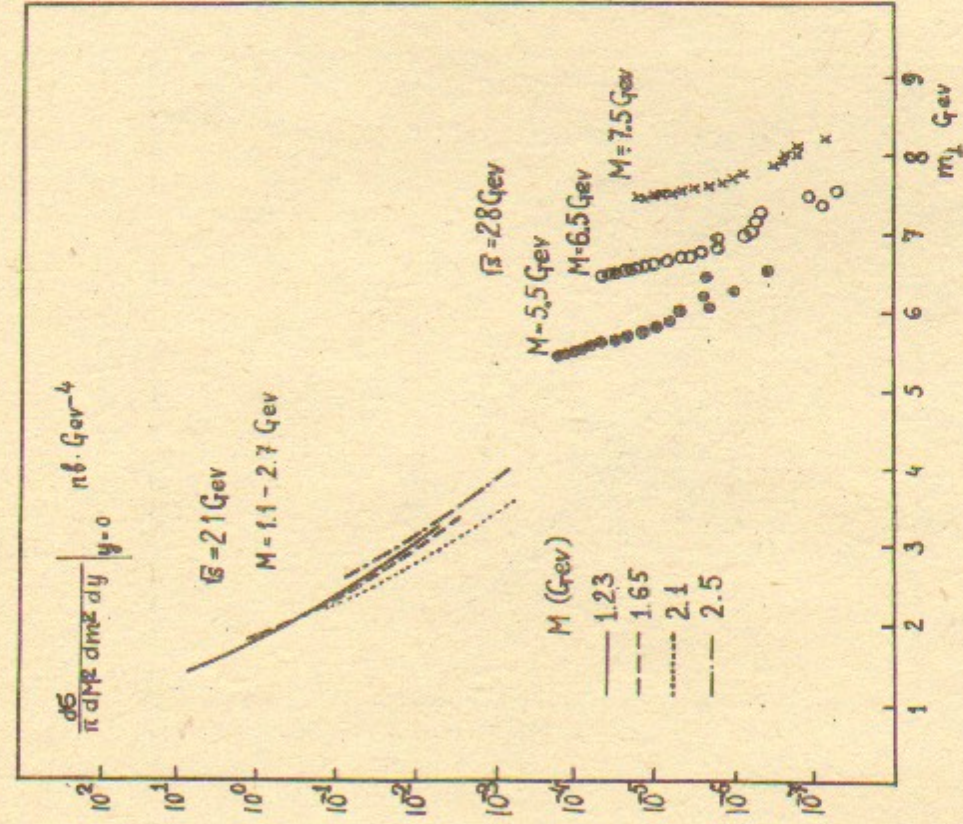


Fig. 3

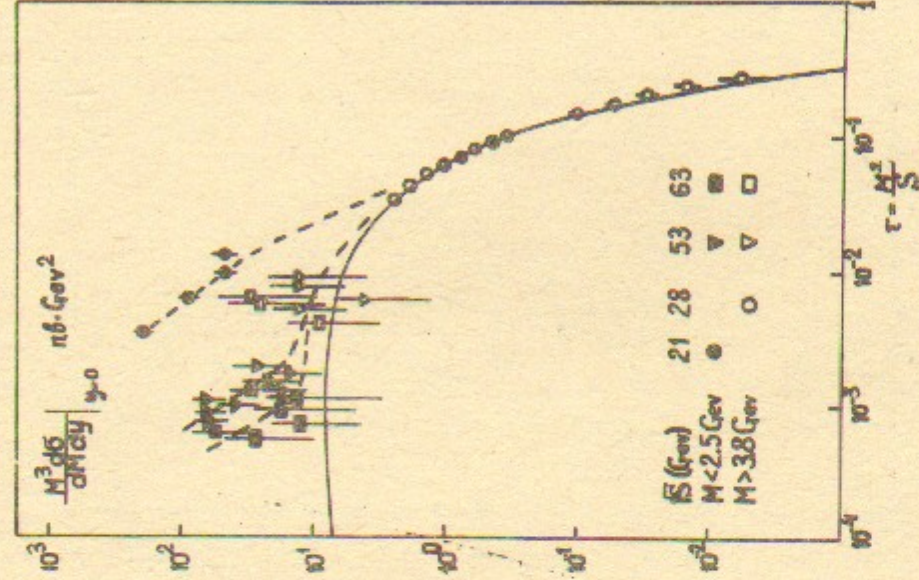


Fig. 4



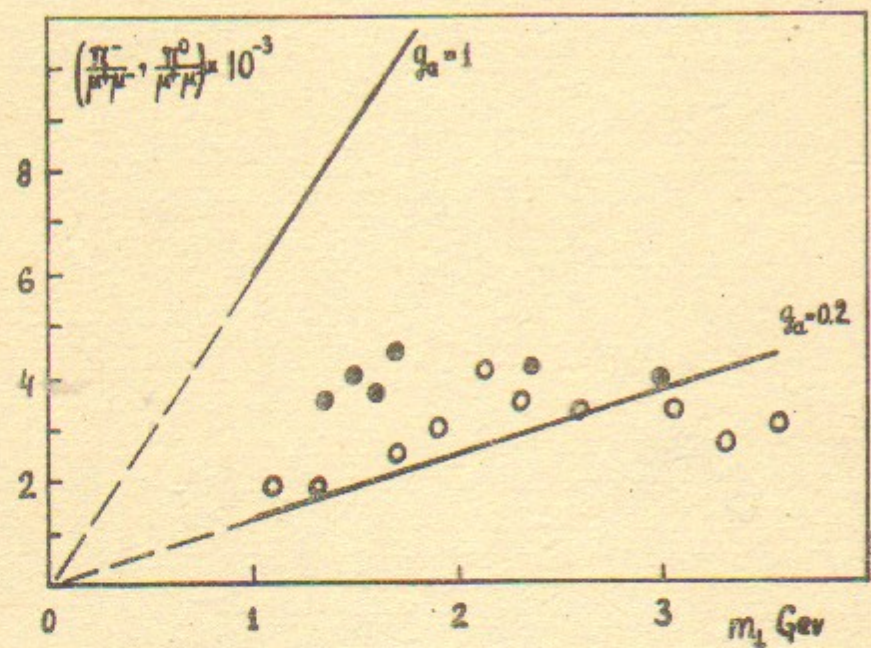


Fig. 5

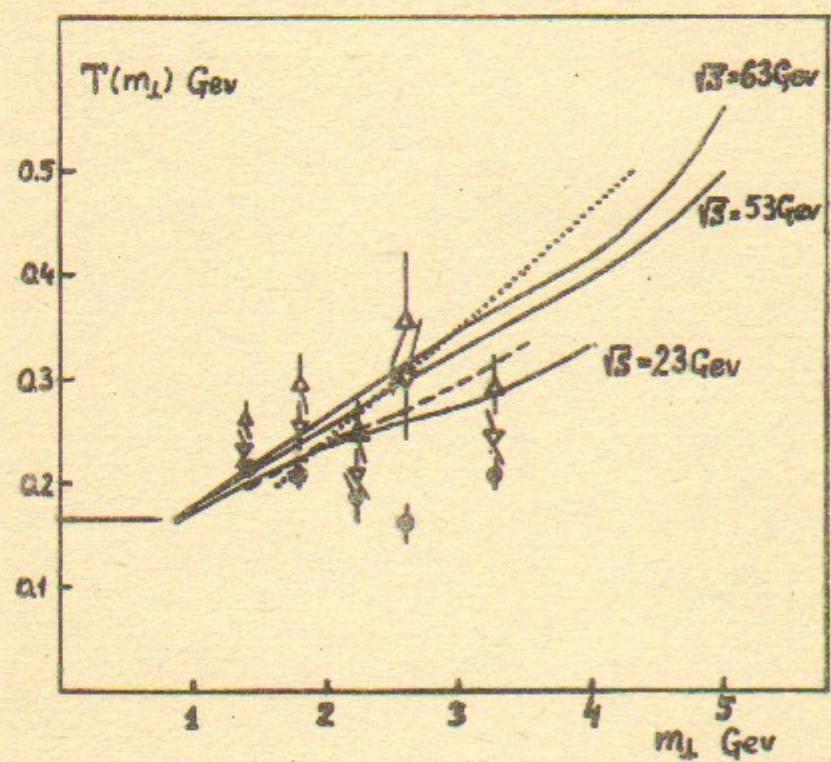


Fig. 6

